ISBN: 978-3-95450-213-4 ISSN: 2673-5490 doi:10.18429/JACoW-IPAC2020-WEVIR16

A NOVEL NONDESTRUCTIVE DIAGNOSTIC METHOD FOR MeV ULTRAFAST ELECTRON DIFFRACTION

X. Yang†, J. Li, M. Fedurin, V. Smaluk, L. Yu, L. Wu, Y. Zhu, T. Shaftan,
Brookhaven National Laboratory, Upton, NY 11973, USA
W. Wan, ShanghaiTech University, Shanghai, China

Abstract

A real-time non-destructive technique to monitor Bragg-diffracted electron beam energy, energy-spread, and spatial-pointing jitter by analysis of the mega-electron-volt ultrafast electron diffraction pattern, is experimentally verified. The shot-to-shot fluctuation of the diffraction pattern is decomposed into two basic modes, i.e., the distance between the Bragg peaks as well as its variation (radial mode) and the overall lateral shift of the whole pattern (drift mode). Since these two modes are completely decoupled, the Bragg-diffraction method can simultaneously measure the shot-to-shot energy fluctuation with $2 \cdot 10^{-4}$ precision and spatial-pointing jitter in the wide range from 10^{-4} to 10^{-1}. The key advantage of this method is the possibility to extract the electron beam energy spread concurrently with the ongoing experiment. This enables the online optimization of the electron beam, especially for future high-charge single-shot ultrafast electron diffraction (UED) and ultrafast electron microscopy (UEM) experiments. Furthermore, the real-time energy measurement enables filtering out off-energy shots, improving the resolution of time-resolved UED. As a result, this method can be applied to the entire UED user community, beyond the traditional electron beam diagnostics used by accelerator physicists.

INTRODUCTION

In recent years, there has been a growing interest in developing single-shot mega-electron-volt (MeV) ultra-fast electron diffraction (UED) systems [1-12]. Comparing to the commonly used electron diffraction in the 100 keV energy range, the main advantages of relativistic electron diffraction are reduced space charge effects and the higher penetration depth. The UED can also resolve much finer structural details compared to X-rays due to the hundreds-fold shorter wavelength of electrons in the required sub-picosecond timescale. However, single-shot imaging with high spatial resolution and small beam size on the sample is a significant challenge and it requires much brighter electron sources. For instance, the RF gun needs to be three orders of magnitude brighter than the present state-of-the-art guns to outrun beam-induced damage of the sample in biomolecular single-particle imaging, achieving “diffraction-before-destruction” [13]. On the other hand, the multi-shot operation requires significantly reduced beam brightness, but with much lower tolerances to the shot-to-shot energy and spatial-pointing fluctuation. To meet these requirements, we need a real-time non-destructive monitor of the electron beam energy and spatial-pointing jitter to characterize the shot-to-shot energy fluctuation and energy spread of the electron beam.

Here we report our proof-of-principle experiment of characterizing the shot-to-shot energy jitter, spatial-pointing jitter, and energy spread of the electron beam for UED and UEM using a novel Bragg-diffraction method (BDM). The experiment was carried out on the existing high-charge high-brightness low-energy electron source developed at Brookhaven National Laboratory (BNL) with the capability of generating 3.3 MeV electron bunches with 10 pC charge (0.62·108 electrons) and 0.1 to 1 ps bunch length [10,11]. We were able to measure simultaneously the shot-to-shot energy fluctuation and spatial-pointing jitter of the electron beam in real-time via eigen-decomposing the variation of the diffraction pattern to two decoupled modes (radial and transverse) and obtain the dispersion of the beamline optics at the detector. Beyond tracking changes of the intensity, position, and width of diffraction patterns [14], we applied the dispersion and Bragg-diffraction (BD) peak width to extract the beam energy spread. The measured beam energy spread agrees reasonably well with Impact-T simulations [15] and with the direct beam-size measurement without crystal diffraction. The non-destructive measurement of the electron beam parameters and beamline optics opens a possibility of online minimization of the shot-to-shot energy jitter, spatial-pointing jitter, and energy spread, which is impossible with the conventional dipole-based diagnostic tools. We have experimentally demonstrated the BDM can provide a nearly complete set of beam-based diagnostic information for online optimization of the RF system stability and minimization of the dispersion at the detector. This is crucial for the future development of single-shot UED and UEM facilities with high-charge electron beam.

EXPERIMENTAL RESULTS

The schematic layout of the UED setup is shown in Figure 1a. The peaks of a BD image shown in Fig. 1b are formed by the summation of the intensity distribution of all diffracted electrons. The diffraction pattern of a single electron is determined by the constructive interference governed by Bragg’s law $2d\sin\theta = n\lambda$, where θ is the incident angle, d is the crystal interplanar distance, λ is the de Broglie wavelength, n is the order of Bragg reflections. For the data analysis, we choose two BD peaks (i and j in Fig. 1b) with the largest separation, highest peak intensities, the same reflection order (ni,j = n) and crystal interplanar distance (di,j = d). Before, we compared the result

† xiyang@bnl.gov

ISBN: 978-3-95450-213-4 ISSN: 2673-5490 doi:10.18429/JACoW-IPAC2020-WEVIR16

from one BD-peak pair (i and j) to the result from two pairs (i and j, k and l) and found them similar. The separation between this highest-intensity peak pair (Dij) is determined by the interplane distance d, the distance between the sample and the detector LS2D and the electron beam energy E:

$$D_{ij}(E,d) = L_{S2D}\cdot \{\tan[2\theta_i(E,d)] - \tan[2\theta_j(E,d)]\} = L_{S2D}\cdot 2\cdot \tan\left[2\sin^{-1}\left(\frac{n\cdot\lambda(E)}{2d}\right)\right] \approx L_{S2D}\cdot\frac{2n\cdot\lambda(E)}{d} \quad (1)$$

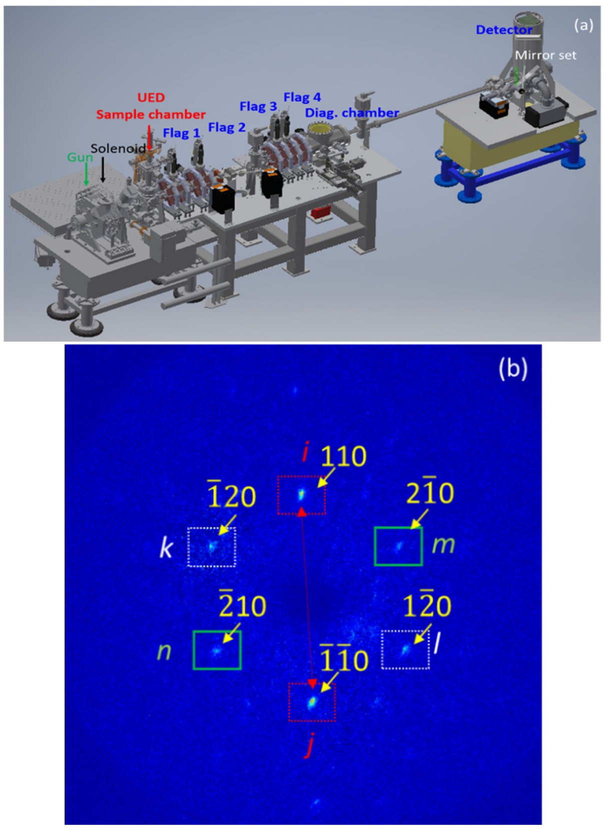

Figure 1: (a) Schematic layout of the UED beamline with marked positions of the UED sample chamber, the YAG screens, and the detector. All the quadrupoles were turned off. (b) Single-shot Bragg diffraction image on the detector. Miller indexes of the Bragg peaks used in data analysis are labelled by yellow colour.

This separation between two BD peaks i and j can be used to measure the electron beam energy and shot-to-shot energy jitter: $\frac{\Delta D_{ij}}{D_{ij}} = \frac{\Delta\lambda}{\lambda} = -\frac{\Delta E}{E}$. The center position of a BD peak can be fitted with precision about 0.05 pixel, which determines the ultimate precision of the energy and energy jitter measurement as 10-4. There is no need for the detailed information of the crystal interplanar distance and the sample-to-detector distance unless one wants to calibrate the absolute beam energy.

There are two basic components associated with the shot-to-shot fluctuation of the BD image. We call the expansion and contraction of the BD image in the radial direction with respect to the image center as the radial mode, and the transverse motion of the whole BD image as the transverse mode. The shot-to-shot energy jitter contributes to the radial mode only, as shown in Figure 2.

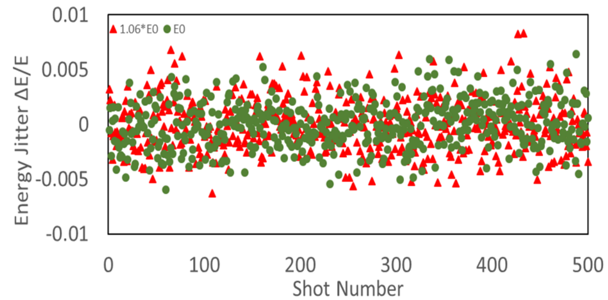

Figure 2: The shot-to-shot energy fluctuation ΔE/E measured at two different beam energies: 0.216% rms at E0 (green) and 0.239% rms at 1.06E0. They are similar.

The transverse mode includes both the spatial-pointing jitter and the dispersive jitter resulted from the combinatory effect of the non-zero dispersion at the detector and the shot-to-shot beam energy fluctuation. The horizontal η_x and vertical η_y dispersion at the detector is caused by the steering from the Earth's magnetic field [10, 11], orbit correctors and the beam off-center at the solenoid. When the beam energy fluctuates shot-to-shot, the non-zero dispersion at the detector results in the transverse motion ΔR of the BD image:

$$R\left(\eta_x,\eta_y,\frac{\Delta E}{E}\right) = \sqrt{\Delta x^2 + \Delta y^2} = \sqrt{\left(\eta_x\cdot\frac{\Delta E}{E}\right)^2 + \left(\eta_y\cdot\frac{\Delta E}{E}\right)^2} = \sqrt{\eta_x{}^2+\eta_y{}^2}\cdot\frac{\Delta E}{E} \quad (2)$$

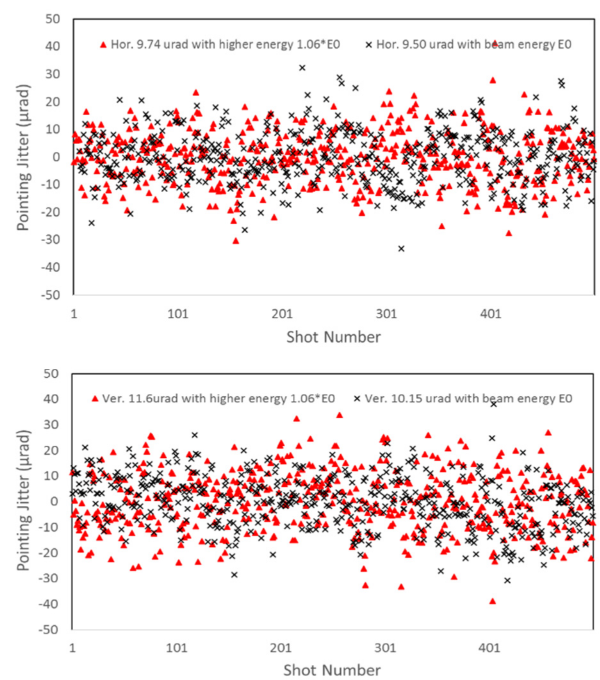

Figure 3: The shot-to-shot pointing jitter measured at two different beam energies: E0 (black) and 1.06E0 (red), the energy jitter is comparably small. The results are similar, about 10 µrad spatial-pointing jitter in both horizontal (top) and vertical (bottom) direction.

If the shot-to-shot energy jitter is small (<0.3% without a slow drift or periodic oscillation), the transverse mode is mainly determined by the spatial-pointing jitter of the UED system (e.g. shot-to-shot laser pointing jitter at the

ISBN: 978-3-95450-213-4 ISSN: 2673-5490 doi:10.18429/JACoW-IPAC2020-WEVIR16

cathode), as shown in Figure 3. However, the spatial-pointing jitter still can be extrapolated from the uncorrelated part of the shot-to-shot 'pointing jitter *vs* energy jitter' dependency, even if the shot-to-shot energy jitter is large. Both cases give similar results, about 10 µrad in both horizontal and vertical directions.

The correlation between the transverse motion of the BD image and the energy jitter can be applied to measure the dispersion. Several sets of data with a large (about 2% peak-to-peak) shot-to-shot energy jitters being were collected and analysed. The overall error of the dispersion measurement is about 6% estimated as $\sqrt{e_1^2 + e_2^2}$. Here the error $e_1 = 0.02$ is caused by the use of different data analysis methods, and $e_2 = 0.06$ is the statistical error. By fitting the pointing jitter vs energy jitter (Fig. 4), we obtain the dispersion $\eta_y \approx 0.0098$ from the equation $\Delta y = \eta_y \cdot \frac{\Delta E}{E}$. Similarly, we obtain $\eta_x \approx 0.004$ with a 10% error.

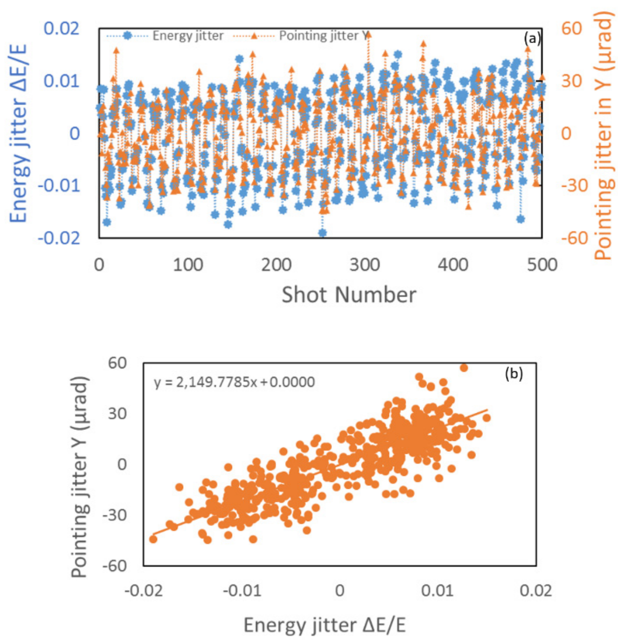

Figure 4: Top: energy jitter (blue, left y-axis) and pointing jitter in y (orange, right y-axis) vs shot number. Bottom: correlation of the pointing jitter and energy jitter.

Different widths σ_x and σ_y of BD peaks are caused by the different dispersions η_x and η_y and the non-zero beam energy spread $\delta E/E$. With the reasonable assumption $\varepsilon_x \approx \varepsilon_y$ and $\beta_x \approx \beta_y$ based on the previous experimental result [10], we can obtain the beam energy spread $\frac{\delta E}{E} = \sqrt{\frac{\sigma_y^2 - \sigma_x^2}{\eta_y^2 - \eta_x^2}}$ using the dispersion measured by the BDM. We compared the energy spread obtained from the measured BD peak widths to the direct beam size measurement without crystal diffraction. The results are consistent and agree reasonably well with Impact-T simulations, as shown in Figure 5. The horizontal error bars come mainly from the laser power fluctuation.

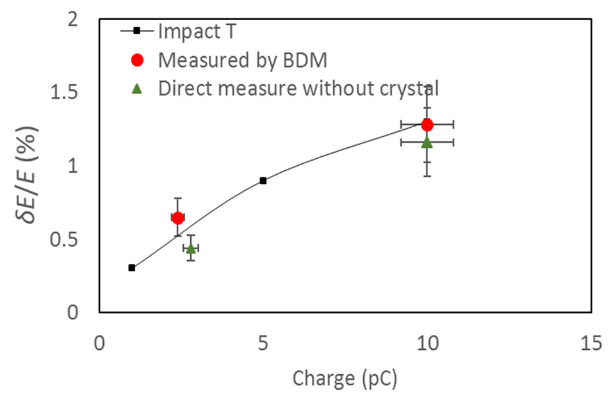

Figure 5: The beam energy spread measured via the BDM (red circles) and direct beam size measurement (green triangles) compared with Impact-T simulations (black squares).

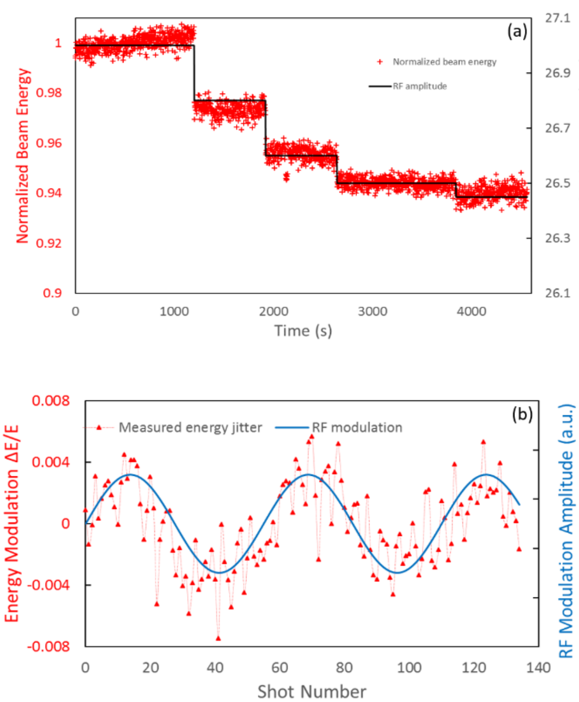

Figure 6: Top: normalized electron beam energy (red, left y-axis) and RF high voltage amplitude (black, right y-axis). Bottom: normalized electron beam energy (red, left y-axis) and LLRF modulator amplitude (blue, right y-axis).

Thus, the BDM can be used to measure the shot-to-shot energy fluctuations, the dispersion, the spatial-pointing jitter, and the beam energy spread. Furthermore, the BDM can be applied to calibrate the electron beam energy in real-time with different RF settings. We measured the beam energy while the RF high-voltage amplitude was varied, the results are shown as Fig. 6a. We also modulated the low-level RF (LLRF) input of the high-voltage amplifier with a sine wave and measured the beam energy variation by the BD method, the result is shown in Fig. 6b. The reason why we chose to vary the beam energy via modulating the amplitude of the LLRF drive signal is that this modulation varies only the RF amplitude not the phase seen by the beam. This feature allows the measurement to be

ISBN: 978-3-95450-213-4 ISSN: 2673-5490 doi:10.18429/JACoW-IPAC2020-WEVIR16

automated because there is no need for the phase correction during the measurement.

CONCLUSION

It is important to monitor the stability of the electron beam non-destructively during the UED experiments. The novel BDM provides an in-situ measurement of the electron beam parameters and beamline optics. Compared to the conventional destructive method based on the beam deflection by a dipole magnet, the unique combination of non-destructiveness and capability of simultaneous measuring the electron beam energy, position and width enables the online optimization of the beam parameters. This is especially important for the future high-charge single-shot UED and UEM development. The dispersion can be measured precisely with a large shot-to-shot energy oscillation. However, if the energy fluctuation is small, we can deliberately introduce an RF modulation with the desired amplitude. The BDM can also be a powerful tool for the RF system diagnostics and troubleshooting. As a further development, we plan to install a quadrupole quadruplet downstream of the mirror reflecting the diffraction pattern to the detector. This mirror has a hole in the center allowing the core of the non-interacted electron beam to pass through and reach the dump. The standard quadrupole scan can provide missing information of the beam emittance to make the online non-destructive diagnostic package complete [16].

REFERENCES

[1] L. Yu, Y. Zhu, T. Shaftan, L. Doom, BNL LDRD # 16-010, 63 (2016). https://www.bnl.gov/ldrd/files/pdf/2016_LDRD_Activities.pdf

[2] P. Zhu, et al., "Femtosecond time-resolved MeV electron diffraction", *New J. of Physics* **17**, 063004 (2015). doi:10.1088/1367-2630/17/6/063004

[3] A. He, F. Willeke, and L. H. Yu, "Ultrashort x-ray pulse generation by electron beam slicing in storage rings", *Phys. Rev. ST Accel. Beams* **17**, 040701 (2014). doi:10.1103/PhysRevSTAB.17.040701

[4] A. He et al., "Design of low energy bunch compressors with space charge effects", Phys. Rev. ST Accel. Beams 18, 014201, (2015). doi:10.1103/PhysRevSTAB.18.014201

[5] J. Yang, et al., "Diffractive imaging of a rotational wavepacket in nitrogen molecules with femtosecond megaelectronvolt electron pulses", *Nat. Commun.* **05**, 11232 (2016). doi:10.1038/ncomms11232

[6] S. P. Weathersby, et al., "Mega-electron-volt ultrafast electron diffraction at SLAC National Accelerator Laboratory", *Rev. Sci. Instrum.* **86**, 073702 (2015). doi:10.1063/1.4926994

[7] F. Fu, et al., "High quality single shot ultrafast MeV electron diffraction from a photocathode radio-frequency gun", *Rev. Sci. Instrum.* **85**, 083701 (2014). doi:10.1063/1.4892135

[8] P. Musumeci, et al., "High quality single shot diffraction patterns using ultrashort megaelectron volt electron beams from a radio frequency photoinjector", *Rev. Sci. Instrum.* **81**, 013306 (2010). doi:10.1063/1.3292683

[9] R. Li, et al., "Experimental demonstration of high quality MeV ultrafast electron diffraction", *Rev. Sci. Instrum.* **80**, 083303 (2009). doi.org/10.1063/1.3194047

[10] Yang, X., Yu, L., Smaluk, V. et al. "A compact tunable quadrupole lens for brighter and sharper ultra-fast electron diffraction imaging", *Sci Rep* **9**, 5115 (2019). doi:10.1038/s41598-019-39208-z

[11] X. Yang et al., "Tuning Quadrupoles for Brighter and Sharper Ultra-fast Electron Diffraction Imaging", in *Proc. 10th Int. Particle Accelerator Conf. (IPAC'19)*, Melbourne, Australia, May 2019, pp. 3571-3573. DOI: 10.18429/JACoW-IPAC2019-THPMP053

[12] W. Wan, F. Chen, and Y. Zhu, "Design of compact ultrafast microscopes for single- and multi-shot imaging with MeV electrons", *Ultramicroscopy* **194**, 143-153 (2018). doi:10.1016/j.ultramic.2018.08.005

[13] J. C. H. Spence, "Outrunning damage: Electrons vs X-rays—timescales and mechanisms", *Struct. Dyn.* 4 (2017) 044027. doi:10.1063/1.4984606

[14] Weathersby et al., "Mega-electron-volt ultrafast electron diffraction at SLAC National Accelerator Laboratory", *Rev. Sci. Instrum.* **86,** 073702 (2015). doi:10.1063/1.4926994

[15] J. Qiang, S. Lidia, R. D. Ryne, C. Limborg-Deprey, "Three-dimensional quasistatic model for high brightness beam dynamics simulation", *Phys. Rev. Special Topics - Accel. Beams* 9, 044204, (2006). doi:10.1103/PhysRevSTAB.9.044204

[16] M. Minty, Diagnostics. CERN Accelerator School, 2004.